Development 139, 1405-1416 (2012) doi:10.1242/dev.070920

Inducible deletion of epidermal *Dicer* and *Drosha* reveals multiple functions for miRNAs in postnatal skin

Monica Teta[1,2,*], Yeon Sook Choi[1,2*], Tishina Okegbe[1,2], Gabrielle Wong[1,2], Oliver H. Tam[3], Mark M. W. Chong[4,‡], John T. Seykora[1], Andras Nagy[5], Dan R. Littman[4], Thomas Andl[6,§] and Sarah E. Millar[1,2,§]

SUMMARY

MicroRNAs (miRNAs) regulate the expression of many mammalian genes and play key roles in embryonic hair follicle development; however, little is known of their functions in postnatal hair growth. We compared the effects of deleting the essential miRNA biogenesis enzymes Drosha and Dicer in mouse skin epithelial cells at successive postnatal time points. Deletion of either *Drosha* or *Dicer* during an established growth phase (anagen) caused failure of hair follicles to enter a normal catagen regression phase, eventual follicular degradation and stem cell loss. Deletion of *Drosha* or *Dicer* in resting phase follicles did not affect follicular structure or epithelial stem cell maintenance, and stimulation of anagen by hair plucking caused follicular proliferation and formation of a primitive transient amplifying matrix population. However, mutant matrix cells exhibited apoptosis and DNA damage and hair follicles rapidly degraded. Hair follicle defects at early time points post-deletion occurred in the absence of inflammation, but a dermal inflammatory response and hyperproliferation of interfollicular epidermis accompanied subsequent hair follicle degradation. These data reveal multiple functions for Drosha and Dicer in suppressing DNA damage in rapidly proliferating follicular matrix cells, facilitating catagen and maintaining follicular structures and their associated stem cells. Although Drosha and Dicer each possess independent non-miRNA-related functions, the similarity in phenotypes of the inducible epidermal *Drosha* and *Dicer* mutants indicates that these defects result primarily from failure of miRNA processing. Consistent with this, *Dicer* deletion resulted in the upregulation of multiple direct targets of the highly expressed epithelial miRNA miR-205.

KEY WORDS: Dicer (Dicer1), Drosha, Skin, miRNA, Hair follicle, Epidermis, Mouse

INTRODUCTION

The epidermis and hair follicles provide an accessible system for studying the molecular mechanisms controlling proliferation, differentiation and maintenance of adult progenitor cells. The interfollicular epidermis (IFE) is composed of a continuously proliferating basal layer, which self-renews and gives rise successively to a non-proliferating suprabasal layer, a granular layer, and a cornified terminally differentiated layer that is cross-linked to form the epidermal barrier (Blanpain and Fuchs, 2009). Hair follicles (HFs) are composed of epithelial cells and a dermal papilla (DP). Throughout postnatal life, HFs undergo cycles of growth (anagen), regression (catagen) and rest (telogen) that depend on a specialized population of label-retaining epithelial stem cells residing in their permanent bulge region (Cotsarelis et al., 1990). At the end of each resting phase, bulge stem cells are stimulated to divide transiently, possibly by signals from dermal cells (Oliver and Jahoda, 1988; Plikus et al., 2008). Bulge cell progeny proliferate rapidly, establishing a matrix population that differentiates to form a keratinized hair shaft (HS) and an inner root sheath (IRS) that molds the HS as it emerges from the skin (Millar, 2002; Fuchs, 2007). An outer root sheath (ORS) that is contiguous with basal epidermis surrounds each follicle.

MicroRNAs (miRNAs) are non-coding RNAs that regulate ~30% of mammalian genes (Lewis et al., 2005). Primary miRNA precursors are transcribed in the nucleus and are processed into 19-22 nt mature miRNAs by the nuclear RNase III enzyme Drosha and its co-factor Dgcr8, and the cytoplasmic RNase III enzyme Dicer. miRNAs bind imperfectly complementary sequences that are usually located in 3′ untranslated regions of target mRNAs, resulting in mRNA degradation and/or translational inhibition (Hendrickson et al., 2009; Djuranovic et al., 2011). The repressive effects of miRNAs on individual target mRNAs are typically relatively mild (Baek et al., 2008; Selbach et al., 2008), and deletion of individual or even multiple related miRNAs often results in subtle phenotypes that sometimes require stress conditions such as tissue injury for their expression.

Although Drosha and Dicer process most miRNAs, the biogenesis of certain miRNA subclasses is either Drosha- or Dicer-independent (Ruby et al., 2007; Cheloufi et al., 2010; Chong et al., 2010; Cifuentes et al., 2010), and both endonucleases also possess miRNA-independent functions (Wu et al., 2000; Tam et al., 2008; Watanabe et al., 2008). Analysis of the effects of *Drosha* or *Dicer* deletion alone might therefore fail to reveal the full scope of miRNA functions or could produce phenotypes unrelated to miRNA processing.

[1]Department of Dermatology, University of Pennsylvania Perelman School of Medicine, Philadelphia, PA 19104, USA. [2]Department of Cell and Developmental Biology, University of Pennsylvania Perelman School of Medicine, Philadelphia, PA 19104, USA. [3]HHMI, Cold Spring Harbor Laboratory, NY 11724, USA. [4]Skirball Institute of Biomolecular Medicine, New York University School of Medicine, New York, NY 10016, USA. [5]Samuel Lunenfeld Research Institute, Mount Sinai Hospital, Toronto M5G 1X5, Ontario, Canada. [6]Division of Dermatology, Department of Medicine, Vanderbilt University Medical Center, Nashville, TN 37232, USA.

*These authors contributed equally to this work
‡Present address: The Walter and Eliza Hall Institute, Parkville, Victoria 3052, Australia
§Authors for correspondence (thomas.andl@vanderbilt.edu; millars@mail.med.upenn.edu)

Accepted 18 January 2012

Approximately seventy miRNAs are expressed in embryonic skin (Andl et al., 2006; Yi et al., 2006). Constitutive epidermal-specific deletion of either *Dicer* or *Dgcr8* during embryonic development causes defects in HF proliferation and HS formation, and evagination, rather than downgrowth, of a subset of HFs (Andl et al., 2006; Yi et al., 2006; Yi et al., 2009). The similarities in these effects suggest that these phenotypes are primarily related to miRNA biogenesis rather than to miRNA-independent functions of Dicer and the Dgcr8-Drosha complex (Yi et al., 2009).

In vitro studies suggest functions for miRNAs in epidermal keratinocyte differentiation (Hildebrand et al., 2011; Xu et al., 2011). miR-205 is highly expressed in epithelia and promotes keratinocyte migration in vitro (Ryan et al., 2006; Yu et al., 2010). Known targets of miR-205 include regulators of proliferation, apoptosis and the epithelial-mesenchymal transition (Gregory et al., 2008; Paterson et al., 2008; Dar et al., 2011; Majid et al., 2011), suggesting possible additional roles for this miRNA in epidermal development and homeostasis. In vivo, overexpression of miR-125b in adult skin results in HF, sebaceous gland and epidermal differentiation defects (Zhang, L. et al., 2011). miR-203 is specifically expressed in suprabasal epidermal cells and its overexpression restricts proliferative potential and suppresses expression of the stem cell-associated transcript *p63* (*Trp63* – Mouse Genome Informatics) (Yi et al., 2008), and miRNA regulation of HF cycling is suggested by the observation of accelerated anagen in mice treated with miR-31 antagomir (Mardaryev et al., 2010).

Given the profound effects of global miRNA depletion on embryonic HF development, and the similar mechanisms that control HF morphogenesis in embryos and cyclical regeneration in the adult (Millar, 2002), we hypothesized that miRNAs play additional key roles in the postnatal HF growth cycle. To test this, we determined the effects of inducible epidermal deletion of *Dicer* (*Dicer1* – Mouse Genome Informatics) or *Drosha* at successive stages of postnatal life. We found that *Dicer* or *Drosha* loss does not affect the maintenance of resting HFs, but produces dramatic defects in cell survival in the rapidly proliferating matrix population during early anagen, blocks transition to a normal regression phase, and prevents long-term maintenance of follicular structures and their associated stem cells. An inflammatory response is observed concomitant with follicular degradation and epidermal hyperplasia, but is preceded by initial HF defects including matrix cell apoptosis and DNA damage. These data demonstrate specific requirements for *Drosha* and *Dicer* in maintaining the ability of adult HFs to undergo normal cycles of growth and regression. The similar phenotypes observed in induced *Drosha* and *Dicer* epidermal mutants suggest that these functions are largely associated with miRNA processing. Consistent with this, *Dicer* deletion resulted in upregulation of multiple direct targets of the highly expressed epithelial miRNA miR-205, which is depleted in *Drosha*- and *Dicer*-deficient skin.

MATERIALS AND METHODS

Mouse strains, Cre induction and wound healing assays

Floxed mice carrying *Krt5-rtTA tetO-Cre* (Zhang et al., 2008) were placed on doxycycline chow (formulated at 6 g/kg chow; Bio-Serv, Laurel, MD, USA) to induce recombination. Genotyping primers are listed in supplementary material Table S1. For specific deletion of *Dicer* in bulge cells, $Dicer^{flEx22\text{-}23/flEx22\text{-}23}$ *ROSA26R* mice carrying the *Krt15-CrePR1* transgene (Ito et al., 2005) were topically treated with 0.1 g Mifepristone (Sigma-Aldrich, St Louis, MO, USA) in ethanol. For wound healing assays, P48 mice were anesthetized with ketamine/xylazine followed by full-thickness excision of a 1 cm^2 area of dorsal skin. All experimental procedures involving mice were performed according to the guidelines of the IACUC committee of the University of Pennsylvania.

Epidermal and HF isolation, qPCR, TUNEL assays, immunofluorescence and in situ hybridization

Separation of epidermis and dermis, HF isolation, qPCR, histological analysis, immunoblotting, CldU and IdU labeling, X-Gal staining, immunostaining and TUNEL assays were performed according to published protocols (Andl et al., 2004; Rendl et al., 2005; Teta et al., 2007; Zhang et al., 2009; LeBoeuf et al., 2010; Andl et al., 2006). Additionally, we used antibodies to Drosha (Bethyl Laboratories, Montgomery, TX, USA); CD34 (Abcam, Cambridge, MA, USA); phospho-H2A.X, Notch1 and Gapdh (Cell Signaling Technology, Danvers, MA, USA); CD11b (Millipore, Billerica, MA, USA); Fgf5 (Santa Cruz Biotechnology, Santa Cruz, CA, USA); and β-actin (Sigma-Aldrich). For in situ hybridization, digoxigenin-labeled LNA probes (Exiqon, Vedbaek, Denmark) were used following the manufacturer's protocol. For proliferation, cell death and DNA damage analyses, 8-30 fields were analyzed at 40× magnification.

RESULTS

miRNAs are depleted in inducible epidermal *Dicer* and *Drosha* mutants

To elucidate the role of *Drosha* and *Dicer* in postnatal HFs and epidermis we paired a conditional *Dicer* allele and two independent conditional *Drosha* alleles with a bi-transgenic *Krt5-rtTA tetO-Cre* system that permits inducible recombination in basal epidermis and HF epithelial cells, including stem cells, on dosage with oral doxycycline (Zhang et al., 2008). The first *Drosha* allele ($Drosha^{flGI}$) contains a floxed gene inactivation cassette (GIC) inserted between exons 3 and 4, upstream of the essential RNase III domains. Cre-mediated recombination promotes irreversible inversion of the GIC (Xin et al., 2005) resulting in premature truncation of *Drosha* mRNA (supplementary material Fig. S1A,B). In the second conditional *Drosha* allele ($Drosha^{flEx9}$), *loxP* sites flank exon 9 and recombination results in a null allele (Chong et al., 2008) (supplementary material Fig. S1C,D). Inducible inactivation of the two *Drosha* alleles produced similar effects, with a slightly less severe phenotype observed for the recombined $Drosha^{flGI}$ allele, possibly owing to splicing of a subset of transcripts around the GIC. The results described below were obtained using the conventional $Drosha^{flEx9}$ allele, except where noted otherwise. In the conditional *Dicer* allele ($Dicer^{flEx22\text{-}23}$), two *loxP* sites flank exons 22 and 23, which encode the majority of the RNase III domain, and Cre recombinase-mediated recombination generates a null mutation (Murchison et al., 2005) (supplementary material Fig. S1E).

Analysis of epidermal genomic DNA from induced *Krt5-rtTA tetO-Cre* $Drosha^{flGI/flGI}$ ($Drosha^{flGI}$ mutant) mice confirmed inversion of the GIC (supplementary material Fig. S1B), and RT-PCR analysis of epidermal mRNA and immunohistochemistry with anti-Drosha antibody showed reduced expression of *Drosha* mRNA and protein in mutants compared with controls (supplementary material Fig. S2A-C). In line with negative regulation of *Dgcr8* by Drosha (Shenoy and Blelloch, 2009), *Dgcr8* mRNA levels were increased in $Drosha^{flGI}$ mutant skin (supplementary material Fig. S2A).

PCR using primers that amplify the recombined $Dicer^{flEx22\text{-}23}$ locus (supplementary material Fig. S1E) confirmed excision in epidermal and HF cells of induced *Krt5-rtTA tetO-Cre* $Dicer^{flEx22\text{-}23/flEx22\text{-}23}$ ($Dicer^{flEx22\text{-}23}$ mutant) mice (supplementary material Fig. S1F,G). Induced $Dicer^{flEx22\text{-}23}$ mutants carrying the

ROSA26R Cre reporter allele showed efficient recombination in epidermal and HF epithelial cells (supplementary material Fig. S1H), and semi-quantitative RT-PCR confirmed decreased *Dicer* mRNA expression in induced *Dicer*$^{flEx22\text{-}23}$ mutant epidermis (supplementary material Fig. S2D).

Consistent with inactivation of *Drosha* and *Dicer*, in situ hybridization and qPCR assays revealed decreased levels of multiple miRNAs in *Dicer*- and *Drosha*-depleted skin, including the highly expressed epithelial miRNA miR-205 (Ryan et al., 2006; Gregory et al., 2008) (Fig. 1A-I; supplementary material Fig. S2E-N).

Drosha or *Dicer* deletion during an established anagen phase reveals essential functions in HF regression and maintenance

To determine whether *Drosha* or *Dicer* is required to maintain anagen or for entry into catagen, *Drosha*^{flEx9} or *Dicer*$^{flEx22\text{-}23}$ deletion was initiated during 'embryonic' anagen at embryonic day (E) 18 or postnatal day (P) 1, and analyzed at successive time points when control littermate HFs were in mid-anagen, catagen or telogen (Fig. 2U). In both mutants, external hair became wavy between P12 and P14 (Fig. 1J,N), followed by hair loss (Fig. 1K,L,O,P), a temporary phenotype of dry scaly skin which resolved in an anterior-posterior direction (Fig. 1L,Q, arrows), and permanent failure of hair regrowth (Fig. 1M,Q). These phenotypes appeared more rapidly in *Dicer* than in *Drosha* mutants, possibly owing to more efficient excision of the *Dicer*$^{flEx22\text{-}23}$ allele and/or the more downstream activity of Dicer relative to Drosha in miRNA biogenesis. Given the faster appearance of overt phenotypes in *Dicer* mutants, further analyses were conducted at slightly earlier stages post-induction in *Dicer* than in *Drosha* mutants. *Drosha*^{flGl}, *Drosha*^{flEx9} and *Dicer*$^{flEx22\text{-}23}$ mutants were generally smaller than littermate controls, which was potentially related to *Krt5* promoter-driven deletion in the forestomach and esophagus (Yagi et al., 2007).

Skin histology revealed abnormal HS structures in *Drosha*^{flEx9} and *Dicer*$^{flEx22\text{-}23}$ mutants compared with littermate controls (Fig. 2A,F,K,P). At P14, when control HFs were in anagen, *Dicer*$^{flEx22\text{-}23}$ mutant follicles displayed elevated numbers of TUNEL-positive cells compared with controls (supplementary material Fig. S3A,B), suggesting that defects in HS formation might result from matrix cell apoptosis.

At P20, despite the presence of apoptotic cells, *Drosha*^{flEx9} and *Dicer*$^{flEx22\text{-}23}$ mutant follicles failed to regress and remained in an abnormal growth phase (Fig. 2G,Q). By contrast, catagen occurred normally in doxycycline-treated control littermates of genotype *Krt5-rtTA tetO-Cre Dicer*$^{+/+}$ and *Krt5-rtTA tetO-Cre Dicer*$^{flEx22\text{-}23/+}$ (Fig. 2B,L; supplementary material Fig. S3C,D), and these controls also showed normal histology at every other stage examined. Expression of Fgf5, a major regulator of the

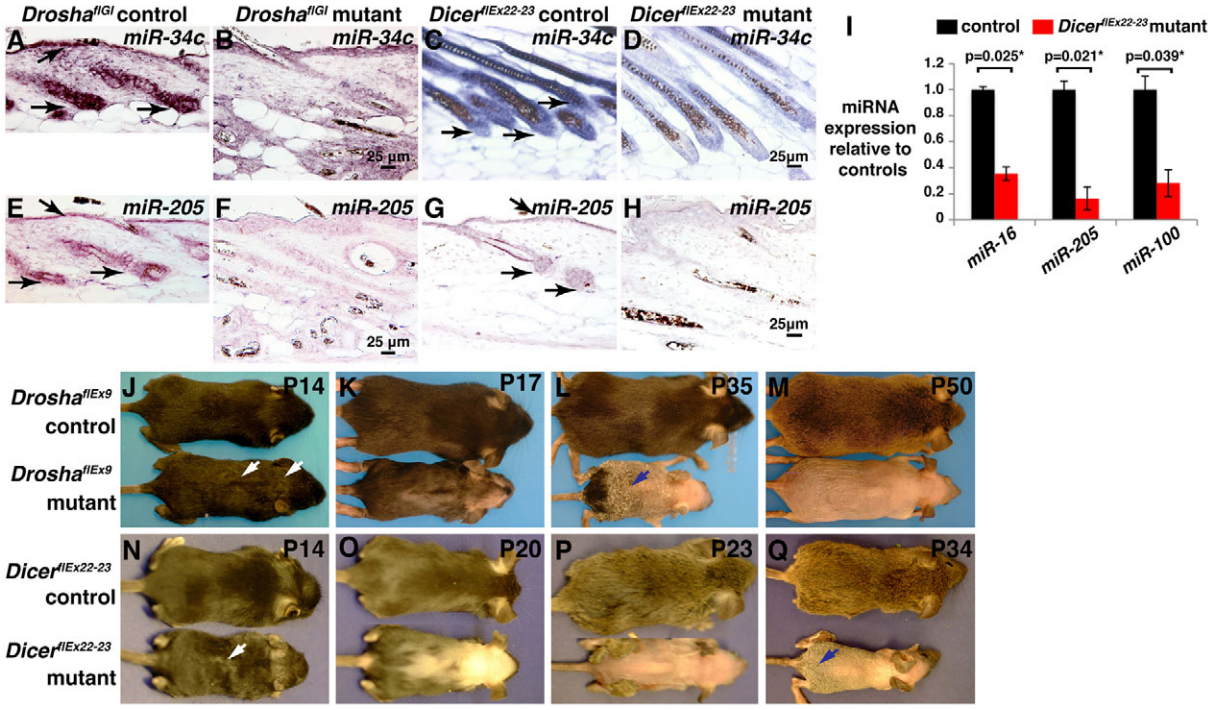

Fig. 1. *Drosha* or *Dicer* deletion in anagen causes miRNA depletion, hair shaft defects and progressive, permanent hair loss. (**A-H**) In situ hybridization for miR-34c (A-D) and miR-205 (E-H) in skin from *Drosha*^{flGl} mutant and control littermate mice that were doxycycline treated from P1 and assayed at P24 (A,B,E,F) and from *Dicer*$^{flEx22\text{-}23}$ mutant and control littermate mice that were doxycycline treated from P1 and assayed at P12 (C,D) or P24 (G,H). Arrows indicate positive signals (purple or blue). Dark brown/black coloration is due to hair pigmentation. Mutant and control pairs were photographed at the same magnification. (**I**) qPCR for the indicated miRNAs using P15 *Dicer*-deleted and control epidermis following doxycycline treatment from P1. miRNA expression was normalized to 4.5S RNA and control mean values were set at 1.0. *P*-values were calculated using a two-tailed Student's *t*-test. Asterisk indicates statistically significant decreases in miRNA levels in *Dicer* mutant compared with control epidermis. Error bars indicate s.e.m. (**J-Q**) *Drosha*^{flEx9} (J-M) and *Dicer*$^{flEx22\text{-}23}$ (N-Q) control (top of each pair) and mutant (bottom of each pair) mice that were doxycycline treated from P1 and photographed at the time points indicated. Wavy hair was noted in both mutants by P14 (J,N, arrows). Hair loss was observed by P17 (K,O) and progressed in an anterior-posterior direction (L,P). Scaly skin was observed transiently (L,Q, arrows) and resolved in an anterior-posterior direction, leaving smooth, permanently hairless skin (M,Q).

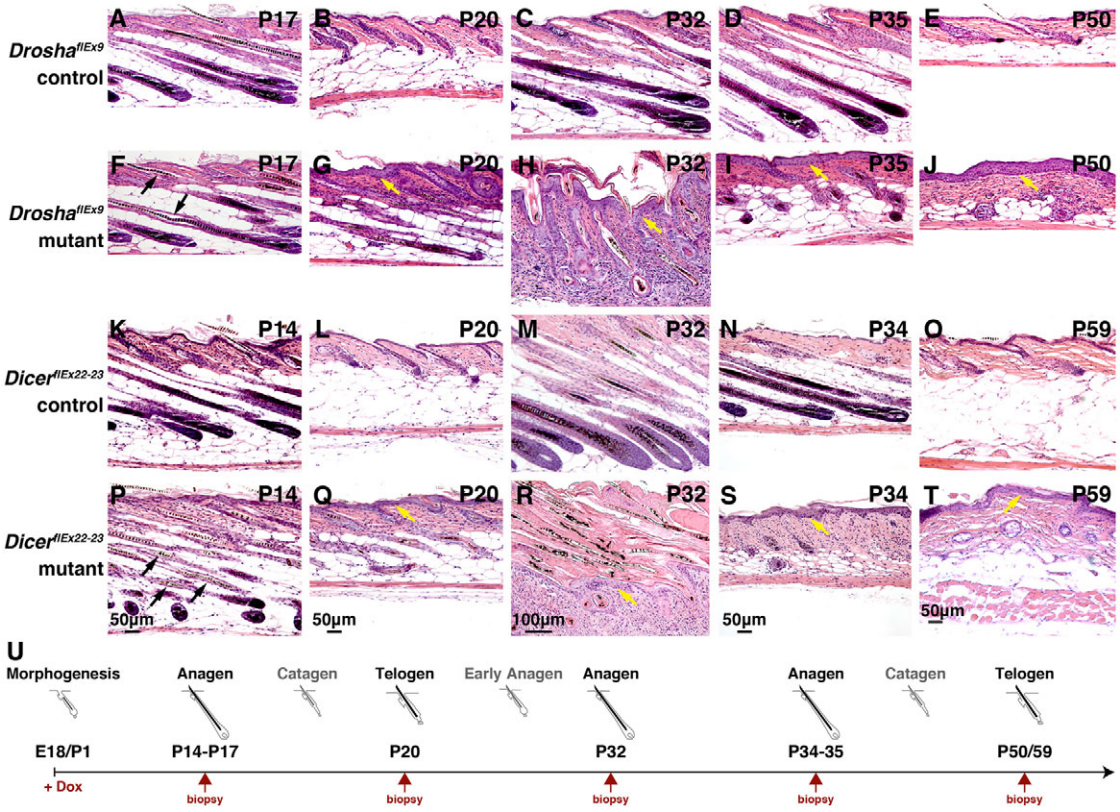

Fig. 2. *Drosha* or *Dicer* deletion during established anagen causes failure of catagen and follicular degradation. (**A-T**) Histology of dorsal skin from *Drosha*^{flEx9} and *Dicer*$^{flEx22-23}$ mutant mice and their control littermates at successive postnatal stages following doxycycline treatment from E18 (*Drosha*^{flEx9}) or P1 (*Dicer*$^{flEx22-23}$). Control hair follicles (HFs) are in anagen at P14-17, telogen at P20, anagen at P32-35, and have re-entered telogen by P50. Irregular hair shafts are apparent in mutants by P14-17 (arrows in F,P). By P20, mutant follicles fail to regress and begin to show signs of degradation, and the interfollicular epidermis (IFE) appears thickened (yellow arrows). At P32, mutants display epidermal scaling and apparent extrusion of abnormally keratinized HF cells (H,R). At P34-35, mutant HFs show increasing signs of degradation (I,S) and by P50-59 only follicle remnants persist (J,T). Scale bars apply to their respective columns. (**U**) Schematic depiction of the embryonic (E18-P20) and first postnatal (P20-59) HF growth cycles indicating time points at which doxycycline administration was initiated and skin was biopsied.

anagen-catagen transition (Hebert et al., 1994), was reduced in P17 *Drosha*^{flEx9} and *Dicer*$^{flEx22-23}$ mutants induced from E18 and P1, respectively, consistent with failure of catagen (supplementary material Fig. S4A-D). *Dicer* deletion induced during the first postnatal anagen phase, starting from P20, produced similar phenotypes to those observed when *Dicer* or *Drosha* was deleted in embryonic anagen (supplementary material Fig. S5A-H).

In both *Drosha*^{flEx9} and *Dicer*$^{flEx22-23}$ mutants, failed catagen was followed by follicular degradation (Fig. 2C,D,H,I,M,N,R,S) and apparent extrusion of abnormally keratinized cellular material from degrading HFs (Fig. 2H,R), consistent with the gross phenotype of epidermal scaling (Fig. 1L,Q). By P50, only HF remnants persisted in mutant skin (Fig. 2E,J,O,T). Krt15-positive stem cells were present in mutant follicles at P20-21 (supplementary material Fig. S4E-H) but were lost by P50-59 (supplementary material Fig. S4I-L). TUNEL staining and expression of the DNA damage response marker pH2A.X in the bulge regions of degrading mutant follicles at P32 (supplementary material Fig. S4M-T) suggested that apoptosis and DNA damage might contribute to stem cell disappearance.

At P17, when *Drosha*^{flEx9} and *Dicer*$^{flEx22-23}$ mutant HFs displayed significant abnormalities, but prior to follicle degradation, mutant and control IFE displayed similar histology, proliferation rates and expression of p63 (Fig. 2A,F,K,P, Fig. 3A-H) and lacked evidence of dermal inflammation (Fig. 3I-L). Importantly, the onset of HF abnormalities in the absence of inflammation indicated that these were a primary consequence of *Drosha* or *Dicer* depletion.

By P20, concomitant with follicular degradation, the IFE became markedly thickened (Fig. 2G-J,Q-T, yellow arrows) and was hyperproliferative at P32 (Fig. 3Q-T), with expanded p63 expression (Fig. 3M-P) and increased numbers of p63-positive cells in Krt10-expressing suprabasal layers (Fig. 3M-P, arrows), consistent with previous results (Yi et al., 2008). By P32, mutant dermis displayed increased numbers of CD11b (Itgam)-positive inflammatory cells, particularly surrounding degrading HFs (Fig. 3U-X).

Given this increase in basal levels of inflammation, we asked whether the inflammatory response to acute wounding was altered in mutant skin by assaying for the presence of CD11b-positive cells 8 days after excision of a 1 cm^2 area of dorsal skin in induced *Drosha*^{flEx9} and *Dicer*$^{flEx22-23}$ mutants and control littermates. All samples displayed increased inflammation compared with unwounded skin. However, the numbers of CD11b-positive cells at wound margins were not statistically different between *Drosha* or *Dicer* mutants and their respective littermate controls (supplementary material Fig. S6).

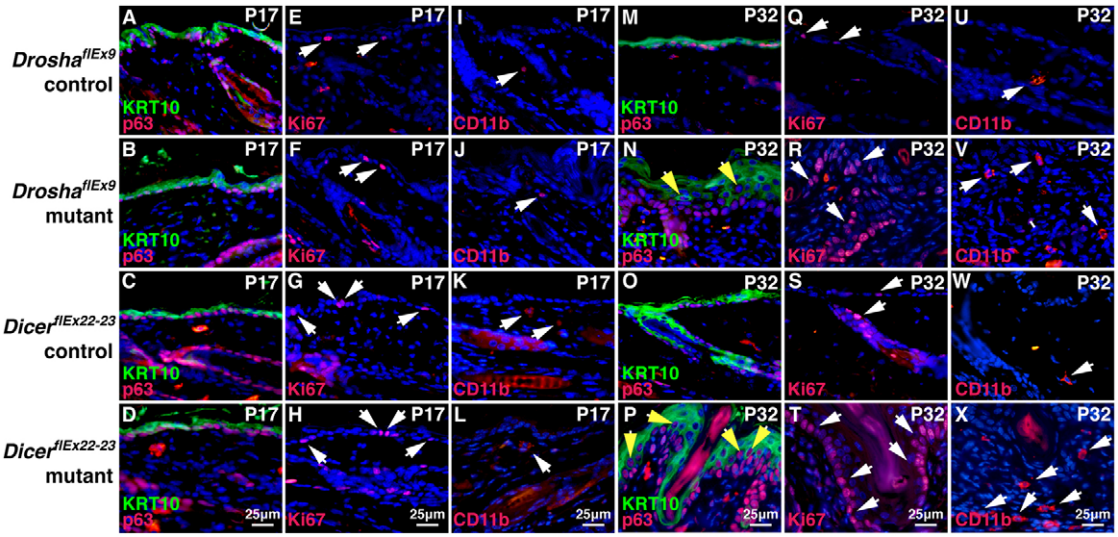

Fig. 3. Delayed onset of epidermal expansion, hyperproliferation and inflammation in *Drosha* and *Dicer* mutant skin. (**A-X**) Immunofluorescence for Krt10 (green) and p63 (red) (A-D,M-P), Ki67 (red) (E-H,Q-T) and CD11b (red) (I-L,U-X) in dorsal skin sections from *Drosha*^{flEx9} and *Dicer*$^{flEx22-23}$ mutants and their control littermates following doxycycline treatment from birth and sacrifice at P17 (A-L) or P32 (M-X). *Drosha* and *Dicer* mutant IFE appears similar to that of controls at P17, but by P32 is thickened and displays expansion of p63-positive cells, increased numbers of cells double-positive for p63 and the suprabasal marker Krt10 (arrows in N,P), hyperproliferation (Q-T, arrows), and an influx of CD11b-positive inflammatory cells (U-X, arrows).

Drosha and *Dicer* are not required for maintenance of stem cells in telogen HFs

To determine whether *Drosha* or *Dicer* is required to maintain resting HFs, *Drosha*^{GI} and *Dicer*$^{flEx22-23}$ mutant mice were induced during the second postnatal telogen and assayed 8-20 days later. Epidermal miRNA levels were depleted following induction in telogen (supplementary material Fig. S7A,B). However, HF structures appeared grossly normal by histological analysis (Fig. 4A-D), Krt15- and CD34-expressing bulge stem cells were maintained (Fig. 4E-H; supplementary material Fig. S8A-D), and TUNEL and pH2A.X staining revealed no increases in apoptosis or DNA damage relative to controls (supplementary material Fig. S8E-L). However, at later time points, after HFs had spontaneously re-entered anagen, degradation of mutant follicular structures and loss of stem cells were observed (Fig. 4I,J). Thus, *Drosha* and *Dicer* are not required for maintenance of stem cells or follicular structures in resting HFs, suggesting that overt defects might be associated with entry into anagen.

Drosha and *Dicer* mutant HFs initiate anagen following hair plucking but fail to sustain normal growth

To test directly whether *Drosha* or *Dicer* mutant follicles become defective upon anagen entry, we induced *Drosha*^{flEx9} and *Dicer*$^{flEx22-23}$ deletion in telogen and initiated a synchronous hair growth cycle by plucking dorsal hair (Fig. 5M). External hair regrowth was observed in littermate controls by 14 days post-plucking (DPP), but was absent in plucked mutant skin. Histological analysis and Ki67 staining at 2 DPP revealed that both control and mutant HFs entered anagen and proliferated in response to plucking

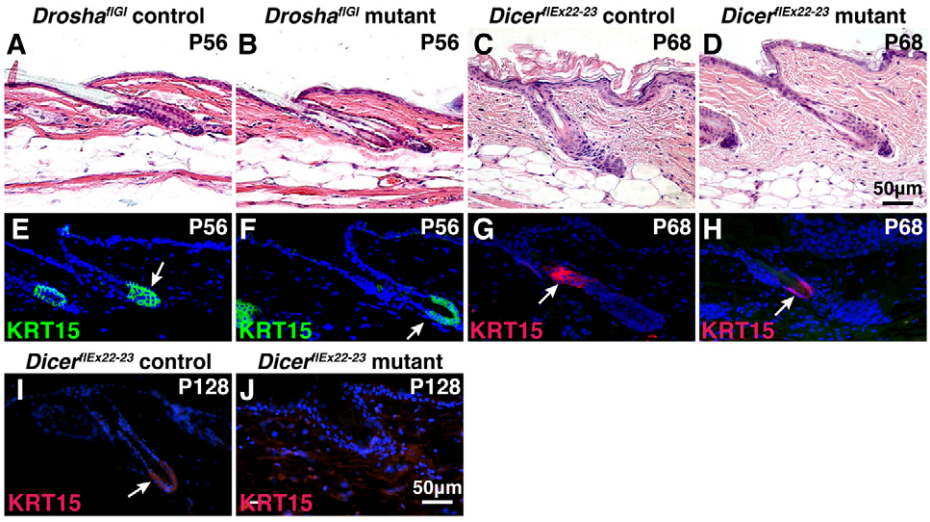

Fig. 4. Krt15-positive stem cells are initially maintained following inactivation of *Drosha* or *Dicer* in telogen but are lost at later stages. (**A**,**B**,**E**,**F**) Dorsal skin from *Drosha*^{flGl} mutants and control littermates induced at P38, biopsied at P56 and analyzed by Hematoxylin and Eosin (H&E) staining (A,B) or immunofluorescence for Krt15 (green) (E,F). (**C**,**D**,**G-J**) Dorsal skin from *Dicer*$^{flEx22-23}$ mutants and control littermates induced at P38, biopsied at P68 (C,D,G,H) or P128 (I,J) and analyzed by H&E staining (C,D) or immunofluorescence for Krt15 (red) (G-J). Sections in E-J were counterstained with DAPI (blue). Arrows indicate positive signals. Scale bar in D applies to A-D; scale bar in J applies to E-J.

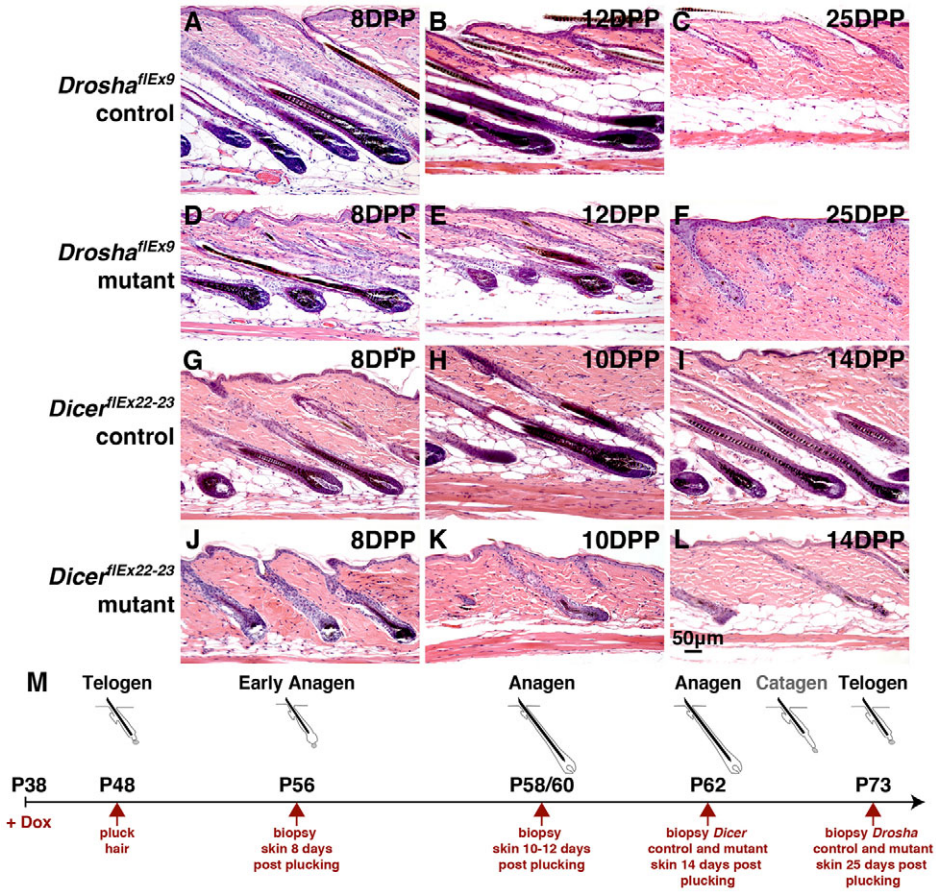

Fig. 5. Anagen defects in *Drosha*^{flEx9} and *Dicer*$^{flEx22-23}$ mutant HFs. (**A-L**) *Drosha*^{flEx9} and *Dicer*$^{flEx22-23}$ mutants and littermate controls were placed on doxycycline at P38, 10 days prior to hair plucking. Skin was biopsied from the lower dorsal region at successive days post-plucking (DPP) as indicated and analyzed by H&E staining. Defects in HF downgrowth were observed in *Drosha* mutants by 12 DPP and in *Dicer* mutants by 8 DPP, and HFs subsequently started to degrade in both mutants. (**M**) Schematic depiction of the plucking-induced HF growth cycle indicating time points at which doxycycline administration was initiated and skin was biopsied.

(supplementary material Fig. S9A-D). However, by 5 DPP, mutant keratinocytes failed to completely surround the DP (supplementary material Fig. S9E-H). The sizes and extent of downgrowth of mutant follicles were reduced by 12 DPP in *Drosha*^{flEx9} and by 8 DPP in *Dicer*$^{flEx22-23}$ mutants as compared with controls (Fig. 5A,B,D,E,G,J; see also supplementary material Fig. S11A,B). In *Dicer*$^{flEx22-23}$ mutant follicles at 8 DPP, the number of DAPI-positive nuclei in the matrix, defined as the region beneath the line of Auber (Peters et al., 2003), was 61±6% of that in control follicles (600-1700 DAPI-positive cells counted per mouse; n=4 controls and n=4 mutants; P=0.0006). The developing HS appeared irregular in both mutants (Fig. 5A,D,G,J). Signs of follicular degradation were observed in *Drosha*^{flEx9} mutants by 12 DPP (Fig. 5B,E) and were marked by 25 DPP (Fig. 5C,F). *Dicer*$^{flEx22-23}$ mutant follicles began to degrade by 10 DPP (Fig. 5H,K) and were atrophic 4 days later (Fig. 5I,L). These data indicate that *Drosha* and *Dicer* are not required for anagen onset. However, both genes are necessary for the early stages of anagen progression, production of external hair and maintenance of early anagen follicles.

Drosha and *Dicer* mutant HF retain stem cells in early anagen

To determine whether loss of bulge stem cells could account for the decreased size of the early anagen matrix in *Drosha*^{flEx9} and *Dicer*$^{flEx22-23}$ mutants, we assayed for expression of the stem cell markers Krt15 and CD34 at 12 or 8 days after plucking, respectively, when mutant follicles showed severe histological defects (Fig. 5B,E,G,J). Interestingly, similar levels of Krt15 and CD34 staining were observed in mutant follicles and littermate controls (Fig. 6A-D; supplementary material Fig. S10A-D). Bulge cells are slow cycling and retain labeled deoxyribonucleotides (Cotsarelis et al., 1990). To determine whether label-retaining cells are affected by *Dicer* deletion, *Dicer*$^{flEx22-23}$ mutant and littermate control mice were injected with chloro-deoxyuridine (CldU) for the first 3 days after birth, and were doxycycline treated from P38, followed by hair plucking at P48. Mice were injected with iodo-deoxyuridine (IdU) to label proliferating cells, 2 hours before skin biopsy at 8 DPP. The numbers of CldU-positive label-retaining cells, IdU-positive proliferating cells, and double-positive proliferating label-retaining cells, as assayed by immunofluorescence, were not significantly different in *Dicer*$^{flEx22-23}$ mutant and control HFs (Fig. 6E-G). Similarly, significant differences were not observed in the numbers or proliferation of Sox9-positive ORS cells, which are necessary for maintenance of the matrix (Nowak et al., 2008), in *Dicer*$^{flEx22-23}$ mutant and control HFs at 3 DPP (Fig. 6H-J). Taken together, these data indicate that loss or failure of proliferation of bulge stem cells and Sox9-positive ORS cells is unlikely to account for matrix defects in early anagen.

Specific deletion of *Dicer* in bulge stem cells does not prevent their contribution to the matrix population

To assay more directly the requirements for miRNAs in early anagen stem cells, we generated *Krt15-CrePR1 Dicer*$^{flEx22-23/flEx22-23}$ *ROSA26R* mice in which deletion of *Dicer* is specifically induced in stem cells by application of topical RU486, and X-Gal staining can be used to track the fates of Cre-active cells and their progeny. Experimental mice and control littermate *Krt15-CrePR1 Dicer*$^{+/+}$ *ROSA26R* mice were treated daily with topical RU486 for 4 days

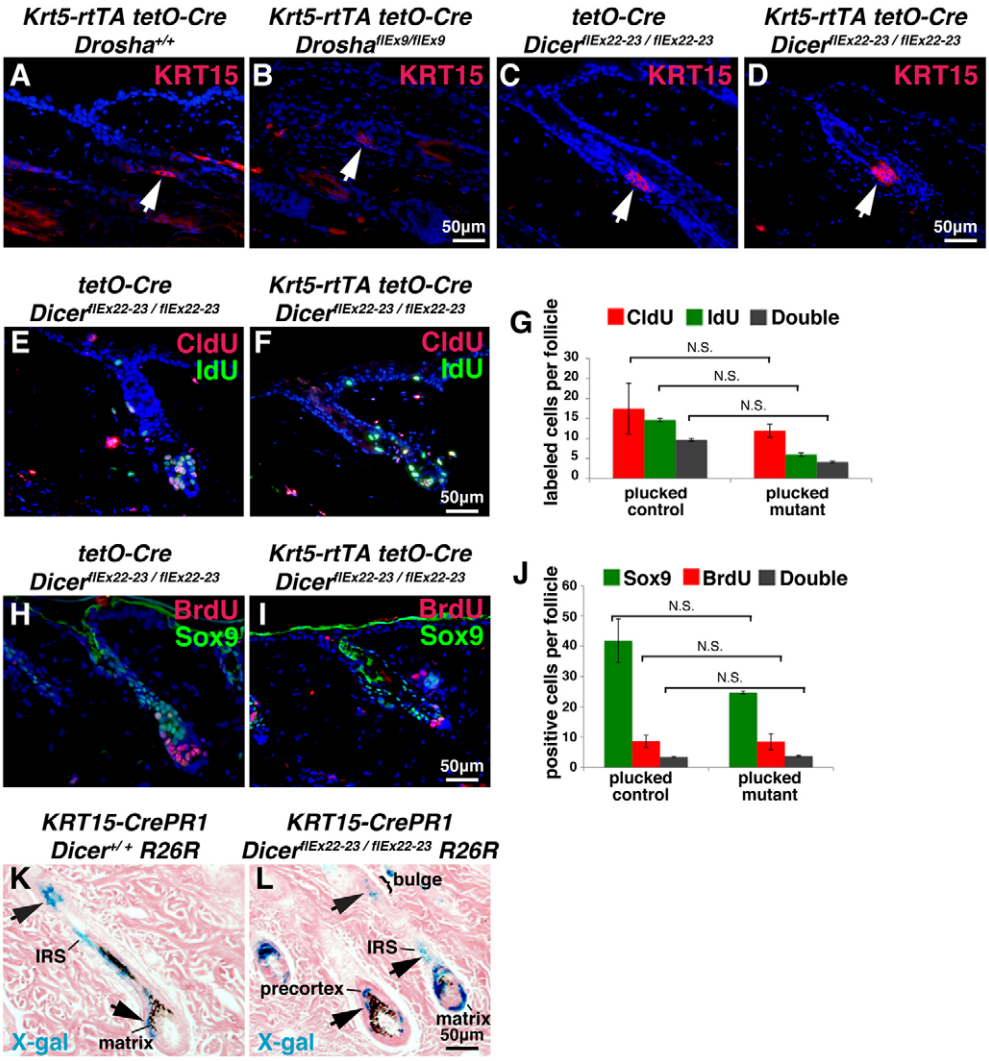

Fig. 6. Maintenance and proliferation of *Drosha*^{flEx9} and *Dicer*$^{flEx22-23}$ mutant HF progenitors in early anagen and contribution of *Dicer*$^{flEx22-23}$ mutant bulge cell progeny to the matrix and its derivatives. (**A-D**) Immunofluorescence for Krt15 (red) in induced *Drosha*^{flEx9} (A,B) and *Dicer*$^{flEx22-23}$ (C,D) control (A,C) and mutant (B,D) skin, 12 (A,B) or 8 (C,D) days after hair plucking. (**E**,**F**) Immunofluorescence for CldU-labeled (red) label-retaining cells and IdU-labeled (green) proliferating cells in induced *Dicer*$^{flEx22-23}$ mutant (F) and control littermate (E) skin at 5 DPP. (**G**) Quantification of the numbers of CldU-labeled, IdU-labeled and double-labeled cells per *Dicer*$^{flEx22-23}$ mutant (I) and control (H) HF section at 5 DPP (n=2 controls and n=3 mutants; more than 6 HFs analyzed per sample). (**H**,**I**) Immunofluorescence for Sox9 (green) and BrdU (red) in *Dicer*$^{flEx22-23}$ mutant and control skin at 3 DPP. (**J**) Quantification of the numbers of BrdU^{+}, Sox9^{+} and co-labeled cells per *Dicer*$^{flEx22-23}$ mutant and control HF section at 3 DPP (n=2 controls and n=2 mutants; more than 6 HFs analyzed per sample). (**K**,**L**) X-Gal-stained dorsal skin from *Krt15-CrePR1 Dicer*$^{flEx22-23/flEx22-23}$ *ROSA26R* (L) and control littermate *Krt15-CrePR1 Dicer*$^{+/+}$ *ROSA26R* (K) mice induced from P46-49, and analyzed 7 days after hair plucking at P50. Arrows indicate Cre-active cells and their progeny in the bulge, matrix, precortex and inner root sheath (IRS). Scale bars apply also to littermate controls. Error bars indicate s.e.m. N.S., not statistically significant.

starting at P46. Hair was plucked at P50 and dorsal skin was biopsied 7 days later. In both mutant and control HFs, mosaic X-Gal staining was observed in the ORS, matrix, precortex and IRS (Fig. 6K,L). These results are consistent with our observation that stem cells are not depleted immediately following *Krt5-rtTA tetO-Cre*-mediated inactivation of *Drosha* or *Dicer*, and suggest that *Dicer*-deleted stem cells can contribute to the matrix and differentiate into HS and IRS.

Drosha and *Dicer* mutant HF matrix cells differentiate appropriately

It was possible that mosaic *Cre* reporter activity did not correlate perfectly with *Dicer* deletion in *Krt15-CrePR1 Dicer*$^{flEx22-23/flEx22-23}$ *ROSA26R* mice. To determine whether Cre-active cells and their progeny could also contribute to HF lineages in the more completely deleted *Krt5-rtTA tetO-Cre* system, we analyzed X-Gal expression in induced *Krt5-rtTA tetO-Cre Dicer*$^{flEx22-23/flEx22-23}$ *ROSA26R* dorsal skin at 8 DPP. X-Gal staining was present in the ORS, IRS and precortex of mutant HFs (supplementary material Fig. S9I,J). Consistent with this, immunofluorescence of *Drosha*^{flEx9} or *Dicer*$^{flEx22-23}$ mutant skin at 12 DPP or 8 DPP, respectively, revealed appropriately compartmentalized expression in mutant follicles of the matrix marker Lef1, the IRS marker Gata3 (Kaufman et al., 2003), the HS marker AE13 (anti-cytokeratin from hair cortex) (Lynch et al., 1986), and AE15 (anti-trichohyalin), which marks IRS and HS medulla cells (O'Guin et al., 1992); however mutant HFs were

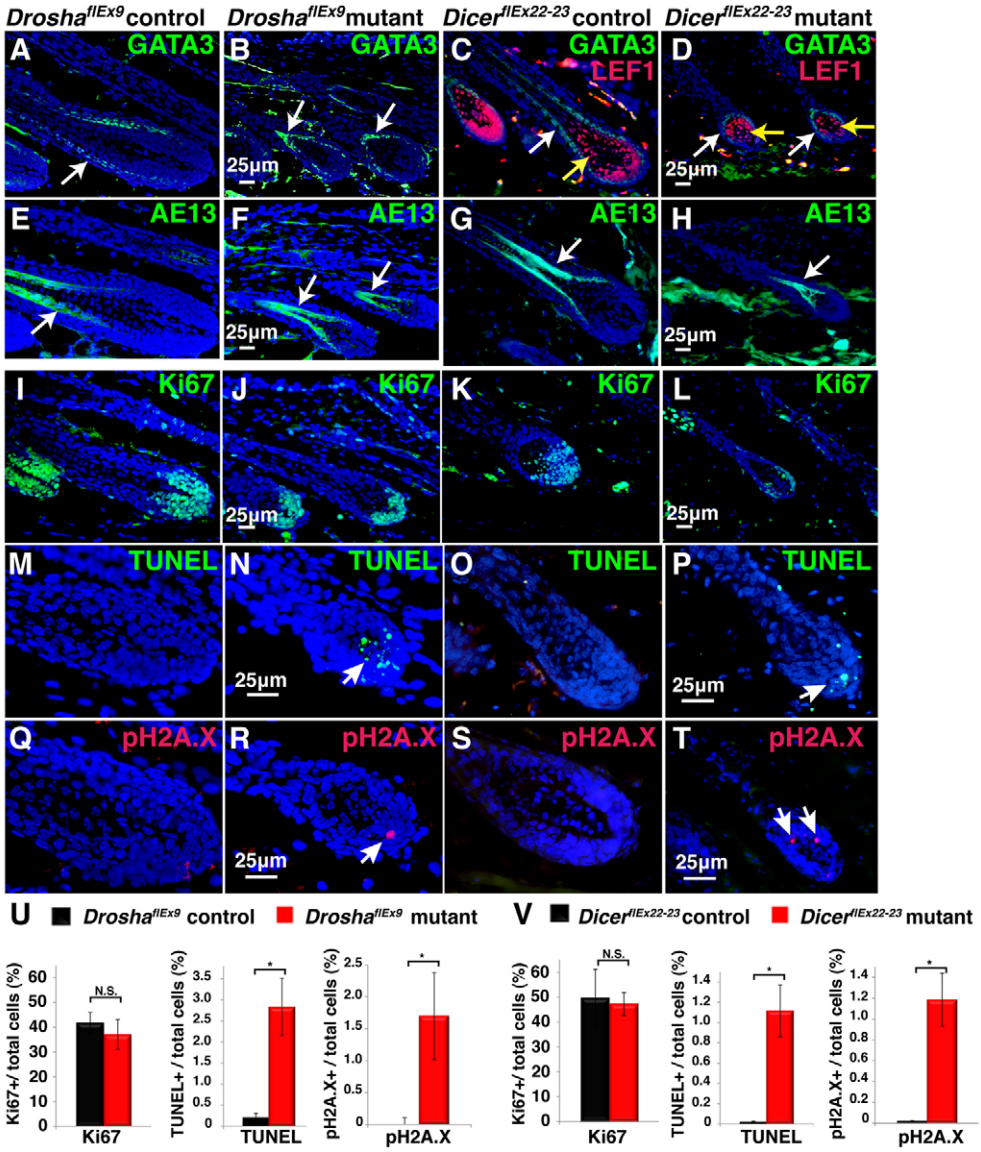

Fig. 7. *Drosha*^{flEx9} and *Dicer*$^{flEx22-23}$ mutant matrix cells differentiate and proliferate normally but display increased rates of apoptosis and DNA damage. (**A-T**) Control littermate and *Drosha*^{flEx9} and *Dicer*$^{flEx22-23}$ mutant mice were placed on doxycycline 10 days prior to hair plucking. Dorsal skin was biopsied 12 days (*Drosha* mutants and controls) or 8 days (*Dicer* mutants and controls) after depilation and assayed by immunofluorescence for Gata3, AE13 or Ki67 (green) and Lef1 or pH2A.X (red) or subjected to TUNEL staining (green) as indicated. White arrows indicate positive signals; yellow arrows indicate Lef1 expression. Scale bars apply also to control littermate images. (**U**,**V**) Percentages of positively staining hair bulb cells, expressed as mean ± s.e.m. for at least eight control and eight mutant follicles (Ki67 staining) or at least 30 control and 30 mutant follicles (TUNEL staining and pH2A.X expression). Both mutants showed statistically significant increases (*P<0.05) in apoptosis and DNA damage relative to controls, but unchanged proliferation rates. NS, not statistically significant.

smaller than controls (supplementary material Fig. S11A,B), contained fewer matrix and differentiating cells, and these did not assemble into normal differentiating structures (Fig. 7A-H; supplementary material Fig. S11A-D).

Dicer and *Drosha* mutant HF matrix cells display normal rates of proliferation

As defective differentiation did not appear to account for *Drosha*^{flEx9} and *Dicer*$^{flEx22-23}$ mutant HF phenotypes, we asked whether *Drosha* or *Dicer* deletion affected proliferation rates. *Drosha*^{flEx9} and *Dicer*$^{flEx22-23}$ mutant hair bulbs contained fewer Ki67-positive cells than littermate controls at 12 DPP and 8 DPP, respectively; however, mutant hair bulbs also contained fewer cells than controls (Fig. 7I-L). Proliferation rates, estimated by calculating the percentage of Ki67-positive DAPI-stained cells in at least eight hair bulbs from control and mutant mice, were not significantly altered by *Drosha* or *Dicer* deletion (*Drosha*^{flEx9} control, 42±4% Ki67-positive cells; *Drosha*^{flEx9} mutant, 37±6%; *Dicer*$^{flEx22-23}$ control, 50±12%; *Dicer*$^{flEx22-23}$ mutant, 47±5%; not statistically significant), indicating that *Drosha* and *Dicer* are not required for normal rates of matrix proliferation (Fig. 7U,V).

Deletion of *Drosha* or *Dicer* causes matrix cell apoptosis and a DNA damage response

We next asked whether the diminished size of *Drosha*^{flEx9} and *Dicer*$^{flEx22-23}$ mutant hair bulbs following hair plucking was due to increased cell death. TUNEL-positive cells were rarely observed in the bulge or matrix of control HFs at 12 DPP or 8 DPP (Fig. 7M,O). By contrast, at 12 DPP and 8 DPP, respectively, *Drosha*^{flEx9} and *Dicer*$^{flEx22-23}$ mutant follicles displayed increased apoptosis, particularly in the matrix (Fig. 7M-P), consistent with elevated *Dicer* mutant matrix cell death in embryonic anagen (supplementary material Fig. S3A,B). At 12 DPP, 2.8±0.7% of *Drosha*^{flEx9} mutant matrix cells were TUNEL positive compared with 0.2±0.1% of control matrix cells (P=0.0003). Likewise, at 8 DPP, 1.1±0.3% of cells were TUNEL positive in *Dicer*$^{flEx22-23}$ mutant follicles compared with 0.020±0.007% in control follicles (P=0.005) (Fig. 7U,V). Interestingly, *Drosha*^{flEx9} and *Dicer*$^{flEx22-23}$ mutant matrix compartments also displayed elevated expression of the DNA damage response marker pH2A.X at 12 DPP and 8 DPP, respectively (Fig. 7Q-T). Quantification of pH2A.X-positive cells as a percentage of the bulb population revealed that these increases were statistically significant (*Drosha*^{flEx9} control 0.0±0.0%,

Drosha^{flEx9} mutant 1.7±0.2%, $P=4.4\times10^{-12}$; *Dicer*$^{flEx22\text{-}23}$ control 0.02±0.01%, *Dicer*$^{flEx22\text{-}23}$ mutant 1.2±0.3%, $P=0.032$) (Fig. 7U,V). These data indicate that *Drosha* and *Dicer* play essential roles in preventing cell death and DNA damage in rapidly proliferating matrix cells during early anagen.

Notch signaling is downregulated and *Tslp* levels are elevated in *Drosha* and *Dicer* mutant skin

Epidermal loss of Notch signaling produces phenotypes similar to those observed following miRNA depletion, including: severe abnormalities at later stages of HF morphogenesis; the ability of *Drosha/Dicer*-depleted and Notch-depleted bulge stem cells to contribute to the matrix, IRS and ORS; failure of HF maintenance; interfollicular epidermal hyperproliferation; and inflammation (Pan et al., 2004; Vauclair et al., 2005; Lee et al., 2007; Demehri et al., 2008; Demehri and Kopan, 2009). Consistent with this, levels of full-length (FL) Notch1 and Notch1 intracellular domain (NICD) were reduced by P17 in *Dicer*$^{flEx22\text{-}23}$ and *Drosha*^{flEx9} mutants compared with control skin following induction from E18 (Fig. 8A,B).

Inflammation in epidermal Notch-deficient mutants is thought to occur as a result of defective barrier formation and is associated with elevated levels of the keratinocyte-derived cytokine Tslp (Demehri et al., 2008). We observed a more than 10-fold elevation in *Tslp* mRNA levels in *Dicer*$^{flEx22\text{-}23}$ mutant compared with control epidermis from mice induced from E18 and biopsied at P15 (Fig. 8C), suggesting that barrier function might be impaired as a result of intrinsic defects in the IFE (Yi et al., 2008) and/or loss of HF integrity. Consistent with these data, treatment of epidermal *Dicer*-depleted mice with MC903, a vitamin D3 analog, triggers increased levels of Tslp production relative to those observed in MC903-treated control mice (Hener et al., 2011). In this latter study, however, epidermal *Dicer*-depleted mice had a normal phenotype in the absence of MC903 treatment, suggesting that *Dicer* deletion was incomplete. Although Tslp levels are directly and positively controlled by miR-375 in intestinal cells (Biton et al., 2011), decreased miR-375 levels in *Dicer*-deficient epidermis and HFs (supplementary material Fig. S2M,N) suggest that epidermal *Tslp* is regulated by other, less direct, mechanisms.

Direct targets of miR-205 are upregulated in *Dicer* mutant skin

To identify direct effects of miRNA depletion on epidermal target mRNAs we focused on miR-205, which is one of the most abundant epithelial miRNAs (Andl et al., 2006; Yi et al., 2006) and is dramatically depleted in epidermal *Drosha* and *Dicer* mutants (Fig. 1E-I; supplementary material Fig. S7). Of particular interest was the direct miR-205 target *E2f1* (Dar et al., 2011), a key regulator of the G1/S transition and p53 (Trp53)-mediated apoptosis (DeGregori, 2002). *Krt5* promoter-driven overexpression of *E2f1* in transgenic mouse skin epithelial cells results in apoptosis of early anagen HF matrix cells and IFE hyperproliferation (Pierce et al., 1998), replicating phenotypes observed in epidermal *Dicer* and *Drosha* mutants. qPCR analysis of dorsal skin samples from P15 *Dicer*$^{flEx22\text{-}23}$ mutants and control littermates induced from E18 revealed a statistically significant increase in the levels of *E2f1* mRNA in mutants relative to controls ($n=2$ mutants and $n=2$ controls; $P=0.038$) (Fig. 8D). These data suggest that miR-205-mediated *E2f1* mRNA degradation might be important in preventing matrix cell apoptosis in early anagen and IFE hyperproliferation.

The transcriptional repressor *Sip1* is another direct target of miR-205 (Paterson et al., 2008) that is elevated in *Dicer*$^{flEx22\text{-}23}$ mutant compared with control skin at P15 in a statistically significant manner ($n=2$ mutants and $n=2$ controls; $P=0.022$) (Fig. 8D). Among other roles, Sip1 regulates the epithelial-mesenchymal transition (Gregory et al., 2008). *Dicer* deletion in embryonic epidermis results in an unusual phenotype of HF evagination (Andl et al., 2006; Yi et al., 2006), and we observed apparent extrusion of keratinized HF cells in induced postnatal epidermal *Drosha* and *Dicer* mutants (Fig. 2H,R). These phenotypes might be related to abnormal control of intercellular adhesion and cell movements by dysregulated *Sip1*.

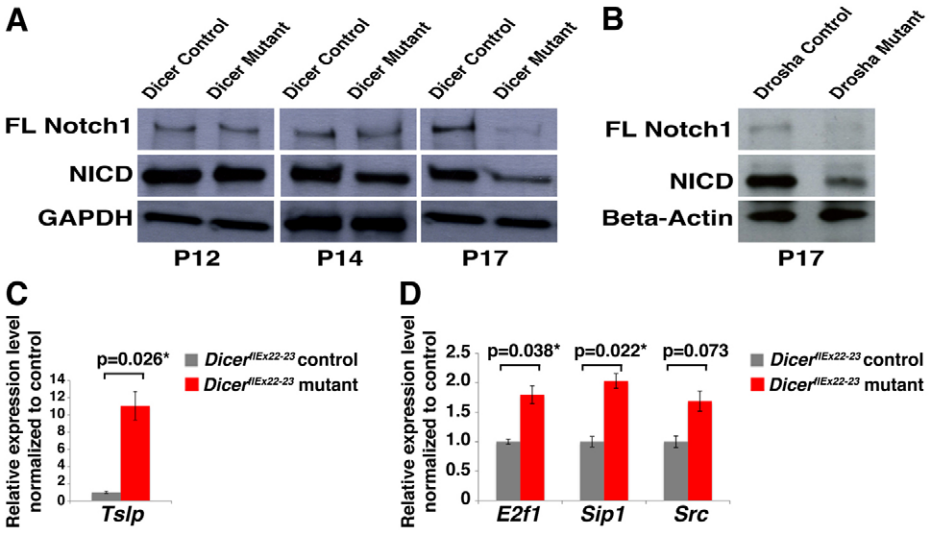

Fig. 8. Decreased levels of full-length Notch1 and NICD and increased expression of *Tslp* and the miR-205 direct targets *E2f1*, *Sip1* and *Src* in miRNA-depleted skin. (**A**,**B**) Immunoblotting for full-length (FL) Notch1, Notch1 intracellular domain (NICD), Gapdh or β-actin using *Dicer*$^{flEx22\text{-}23}$ (A) and *Drosha*^{flEx9} (B) mutant and littermate control skin extracts at the time points indicated, following doxycycline treatment from E18. (**C**,**D**) qPCR analyses of *Tslp* (C) or *E2f1*, *Sip1* and *Src* (D) mRNAs extracted from P15 *Dicer*$^{flEx22\text{-}23}$ mutant and control skin following doxycycline treatment from E18 ($n=2$ control and $n=2$ mutant samples for each experiment; qPCR replicated three times for each sample). Control expression levels were normalized to 1.0. Relative expression levels are shown (arbitrary units). *P*-values were calculated using a two-tailed Student's *t*-test. Asterisks indicate statistically significant differences.

A third direct miR-205 target, the non-receptor intracellular tyrosine kinase Src (Majid et al., 2011), was also upregulated in *Dicer* mutant skin, although this did not reach statistical significance (n=2 mutants and n=2 controls; P=0.073) (Fig. 8D). Elevated levels of epidermal Src cause hyperproliferation, HF defects and chronic inflammation (Matsumoto et al., 2003; Yagi et al., 2007) and could contribute to these abnormalities in miRNA-depleted skin.

Taken together, these results suggest that upregulation of multiple miRNA target genes contributes to the complex phenotypes of epidermal *Drosha* and *Dicer* mutants.

DISCUSSION

Here we use inducible epidermal-specific deletion of two independent components of the miRNA biogenesis pathway, Drosha and Dicer, to investigate the global functions of miRNAs at successive stages of the postnatal HF growth cycle and in adult epidermis. HF and epidermal phenotypes resulting from postnatal epidermal depletion of Drosha and Dicer were virtually identical at each stage examined, suggesting that miRNA-independent functions of these enzymes play only minor roles in postnatal HFs and epidermis. A similar conclusion was reached following comparison of the effects of Dgcr8 and Dicer depletion in embryonic skin (Yi et al., 2009). Thus, it seems likely that the expression of co-factors that modulate the actions of Drosha-Dgcr8 and Dicer in the epidermis does not change substantially after birth. The largely miRNA-related functions of the Drosha-Dgcr8 complex and Dicer in skin epithelial cells at multiple developmental and postnatal stages contrast with the prominent miRNA-independent roles of these enzymes in certain other cell types, such as early-stage thymocytes (Chong et al., 2010), but are similar to what has been observed in regulatory T-cells (Chong et al., 2008).

Dicer deletion in epidermal cells during embryonic development leads to a failure in establishment of the HF bulge stem cell compartment (Andl et al., 2006). Interestingly, however, deletion of either *Drosha* or *Dicer* in established, resting, telogen stage HFs did not cause marked histological abnormalities or loss of HF stem cells prior to entry into a natural or depilation-induced anagen stage. Thus, miRNAs are required for establishment of the HF stem cell compartment, but not for its maintenance in resting follicles.

In contrast to the lack of gross abnormalities during the resting phase, mutant HFs were unable to engage in normal growth. HF stem and matrix cells in either mutant proliferated following plucking, and stem cells were not initially depleted in mutant follicles. However, matrix cells exhibited marked increases in cell death that led to failed HF downgrowth and rapid follicular degradation. Interestingly, matrix cell death in *Drosha* and *Dicer* mutants was accompanied by a DNA damage response, indicated by a significantly increased percentage of cells expressing the DNA damage marker pH2A.X compared with controls. At early stages following deletion, pH2A.X expression was specific to matrix cells; however, once HFs started to degrade, apoptosis and a DNA damage response were also observed in the bulge.

Initiation of *Drosha* or *Dicer* deletion in established anagen HFs also resulted in matrix cell apoptosis and defective HS assembly. Strikingly, HFs were maintained in an abnormal proliferative state instead of undergoing programmed regression, revealing essential functions for miRNAs in the anagen-catagen transition. Expression of Fgf5, a key regulator of catagen (Hebert et al., 1994), was reduced in mutant follicles at this stage. As most direct miRNA targets are predicted to be upregulated following *Drosha* or *Dicer* deletion, it is likely that an inhibitor of *Fgf5* expression, rather than *Fgf5* itself, is a direct target of miRNA action during catagen.

Failed catagen in *Drosha* and *Dicer* mutants was followed by follicular degradation, an inflammatory response and epidermal hyperplasia. Defects in mutant HFs, including HS abnormalities and failure of regression, were observed soon after induction of *Drosha* or *Dicer* gene inactivation and prior to the appearance of an inflammatory infiltrate, indicating that these were caused directly by miRNA depletion and were not a consequence of inflammation.

By contrast, epidermal hyperproliferation in *Drosha* and *Dicer* mutants was concomitant with inflammation. This suggests that degrading HFs trigger a dermal inflammatory response and might cause breaks in the epidermal barrier, further promoting inflammation and IFE hyperproliferation. In addition, IFE-intrinsic mechanisms associated with miRNA depletion could contribute to IFE hyperplasia and inflammation. These mechanisms include loss of direct repression of *p63* by miR-203 (Yi et al., 2008; Lena et al., 2008), depletion of the cell cycle-inhibitory miRNAs miR-34a and miR-34c (Antonini et al., 2010), decreased Notch signaling, and possibly increased levels of Src tyrosine kinase. Whether depletion of miRNAs contributes directly or indirectly to decreased levels of Notch1 and Notch1 NICD in *Drosha* and *Dicer* mutants, and enhances susceptibility to tumorigenesis as is seen in Notch pathway mutants (Demehri et al., 2009b), will be important areas for future investigation.

The delay in the appearance of IFE phenotypes relative to HF defects might be due to the relatively slow turnover of IFE cells compared with the HF matrix. As there is extensive cross-talk between skin epithelial cells, dermal fibroblasts and skin adipose tissue (Plikus et al., 2008; Festa et al., 2011), additional secondary effects of epithelial miRNA depletion on dermal and adipose cells, including activation of stromal fibroblasts (Demehri et al., 2009a), might contribute to epidermal phenotypes in *Drosha* and *Dicer* mutants.

The most immediate and striking phenotypes in *Drosha* or *Dicer* mutants were observed in the early anagen HF matrix, one of the most rapidly proliferating adult cell populations, which displayed increased apoptosis and DNA damage. The extremely rapid proliferation of matrix cells might render them particularly susceptible to double-stranded breaks, resulting in increased requirements for genomic repair. We observed increased expression of the direct miR-205 target *E2f1*, a key regulator of the G1/S transition and p53-mediated apoptosis (Dar et al., 2011), in *Dicer* mutant skin. Interestingly, forced expression of *E2f1* in transgenic mouse skin epithelial cells causes a similar phenotype of HF matrix cell apoptosis and IFE hyperproliferation (Pierce et al., 1998), suggesting that miR-205-mediated *E2f1* mRNA degradation might be important in preventing matrix cell apoptosis in early anagen and IFE hyperplasia. E2f1 is post-translationally modified in response to DNA damage, localizes to DNA strand breaks, recruits repair factors and promotes DNA repair (Degregori, 2011), and thus might also contribute to the abnormal DNA damage response observed in miRNA-depleted matrix cells.

Another possible mechanism contributing to our observation of elevated phosphorylated histone H2A.X in mutant matrix cells is decreased production of miR-24, which is known to directly target the *H2ax* (*H2afx* – Mouse Genome Informatics) transcript (Lal et al., 2009). In addition, accumulating data suggest key roles for miRNAs in the DNA damage response (Hu et al., 2010; Leung and Sharp, 2010; Hu and Gatti, 2011). Biogenesis of a subset of miRNAs is markedly upregulated in an Atm-dependent fashion following DNA damage (Zhang, X. et al., 2011; Suzuki et al., 2009). Atm controls miRNA biogenesis through phosphorylation of KH-type splicing

regulatory protein (Ksrp; Khsrp – Mouse Genome Informatics), which associates with both Drosha and Dicer, facilitating recruitment and processing of specific miRNA precursors (Liu and Liu, 2011). Other, Ksrp-independent miRNAs, such as miR-34a/c, are transcriptionally upregulated by p53 in response to DNA damage (He et al., 2007). The functions of DNA damage-induced miRNAs have been suggested to include facilitating DNA repair, cell cycle arrest and apoptosis; alternatively, they could act in a negative-feedback loop to dampen the DNA damage response once repair is completed (Liu and Liu, 2011). Our data showing increased apoptosis and pH2A.X levels in *Drosha*- and *Dicer*-depleted matrix cells are consistent with the latter role. The identification and functional analysis of the individual miRNAs and their targets that are important for suppressing the DNA damage response in matrix cells are likely to provide mechanistic insights into this process that are relevant well beyond the HF.

Acknowledgements
We thank Adam Glick (Pennsylvania State University) for *Krt5-rtTA* mice, Gregory Hannon (Cold Spring Harbor Laboratory) for *Drosha*^{GI} mice, and Leroy Ash for histology.

Funding
This work was supported by the National Institutes of Health [RO1AR055241 to S.E.M. and the Penn Skin Diseases Research Center P30AR057217]; M.T. was supported by T32AR007465. Deposited in PMC for release after 12 months.

Competing interests statement
The authors declare no competing financial interests.

Supplementary material
Supplementary material available online at
http://dev.biologists.org/lookup/suppl/doi:10.1242/dev.070920/-/DC1

References

Andl, T., Ahn, K., Kairo, A., Chu, E. Y., Wine-Lee, L., Reddy, S. T., Croft, N. J., Cebra-Thomas, J. A., Metzger, D., Chambon, P. et al. (2004). Epithelial Bmpr1a regulates differentiation and proliferation in postnatal hair follicles and is essential for tooth development. *Development* **131**, 2257-2268.
Andl, T., Murchison, E. P., Liu, F., Zhang, Y., Yunta-Gonzalez, M., Tobias, J. W., Andl, C. D., Seykora, J. T., Hannon, G. J. and Millar, S. E. (2006). The miRNA-processing enzyme dicer is essential for the morphogenesis and maintenance of hair follicles. *Curr. Biol.* **16**, 1041-1049.
Antonini, D., Russo, M. T., De Rosa, L., Gorrese, M., Del Vecchio, L. and Missero, C. (2010). Transcriptional repression of miR-34 family contributes to p63-mediated cell cycle progression in epidermal cells. *J. Invest. Dermatol.* **130**, 1249-1257.
Baek, D., Villen, J., Shin, C., Camargo, F. D., Gygi, S. P. and Bartel, D. P. (2008). The impact of microRNAs on protein output. *Nature* **455**, 64-71.
Biton, M., Levin, A., Slyper, M., Alkalay, I., Horwitz, E., Mor, H., Kredo-Russo, S., Avnit-Sagi, T., Cojocaru, G., Zreik, F. et al. (2011). Epithelial microRNAs regulate gut mucosal immunity via epithelium-T cell crosstalk. *Nat. Immunol.* **12**, 239-246.
Blanpain, C. and Fuchs, E. (2009). Epidermal homeostasis: a balancing act of stem cells in the skin. *Nat. Rev. Mol. Cell Biol.* **10**, 207-217.
Cheloufi, S., Dos Santos, C. O., Chong, M. M. and Hannon, G. J. (2010). A dicer-independent miRNA biogenesis pathway that requires Ago catalysis. *Nature* **465**, 584-589.
Chong, M. M., Rasmussen, J. P., Rudensky, A. Y. and Littman, D. R. (2008). The RNase III enzyme Drosha is critical in T cells for preventing lethal inflammatory disease. *J. Exp. Med.* **205**, 2005-2017.
Chong, M. M., Zhang, G., Cheloufi, S., Neubert, T. A., Hannon, G. J. and Littman, D. R. (2010). Canonical and alternate functions of the microRNA biogenesis machinery. *Genes Dev.* **24**, 1951-1960.
Cifuentes, D., Xue, H., Taylor, D. W., Patnode, H., Mishima, Y., Cheloufi, S., Ma, E., Mane, S., Hannon, G. J., Lawson, N. D. et al. (2010). A novel miRNA processing pathway independent of Dicer requires Argonaute2 catalytic activity. *Science* **328**, 1694-1698.
Cotsarelis, G., Sun, T. T. and Lavker, R. M. (1990). Label-retaining cells reside in the bulge area of pilosebaceous unit: implications for follicular stem cells, hair cycle, and skin carcinogenesis. *Cell* **61**, 1329-1337.
Dar, A. A., Majid, S., de Semir, D., Nosrati, M., Bezrookove, V. and Kashani-Sabet, M. (2011). miRNA-205 suppresses melanoma cell proliferation and induces senescence via regulation of E2F1 protein. *J. Biol. Chem.* **286**, 16606-16614.
DeGregori, J. (2002). The genetics of the E2F family of transcription factors: shared functions and unique roles. *Biochim. Biophys. Acta* **1602**, 131-150.
Degregori, J. (2011). A new role for E2F1 in DNA repair: all for the greater good. *Cell Cycle* **10**, 1716.
Demehri, S. and Kopan, R. (2009). Notch signaling in bulge stem cells is not required for selection of hair follicle fate. *Development* **136**, 891-896.
Demehri, S., Liu, Z., Lee, J., Lin, M. H., Crosby, S. D., Roberts, C. J., Grigsby, P. W., Miner, J. H., Farr, A. G. and Kopan, R. (2008). Notch-deficient skin induces a lethal systemic B-lymphoproliferative disorder by secreting TSLP, a sentinel for epidermal integrity. *PLoS Biol.* **6**, e123.
Demehri, S., Morimoto, M., Holtzman, M. J. and Kopan, R. (2009a). Skin-derived TSLP triggers progression from epidermal-barrier defects to asthma. *PLoS Biol.* **7**, e1000067.
Demehri, S., Turkoz, A. and Kopan, R. (2009b). Epidermal Notch1 loss promotes skin tumorigenesis by impacting the stromal microenvironment. *Cancer Cell* **16**, 55-66.
Djuranovic, S., Nahvi, A. and Green, R. (2011). A parsimonious model for gene regulation by miRNAs. *Science* **331**, 550-553.
Festa, E., Fretz, J., Berry, R., Schmidt, B., Rodeheffer, M., Horowitz, M. and Horsley, V. (2011). Adipocyte lineage cells contribute to the skin stem cell niche to drive hair cycling. *Cell* **146**, 761-771.
Fuchs, E. (2007). Scratching the surface of skin development. *Nature* **445**, 834-842.
Gregory, P. A., Bert, A. G., Paterson, E. L., Barry, S. C., Tsykin, A., Farshid, G., Vadas, M. A., Khew-Goodall, Y. and Goodall, G. J. (2008). The miR-200 family and miR-205 regulate epithelial to mesenchymal transition by targeting ZEB1 and SIP1. *Nat. Cell Biol.* **10**, 593-601.
He, L., He, X., Lim, L. P., de Stanchina, E., Xuan, Z., Liang, Y., Xue, W., Zender, L., Magnus, J., Ridzon, D. et al. (2007). A microRNA component of the p53 tumour suppressor network. *Nature* **447**, 1130-1134.
Hebert, J. M., Rosenquist, T., Gotz, J. and Martin, G. R. (1994). FGF5 as a regulator of the hair growth cycle: evidence from targeted and spontaneous mutations. *Cell* **78**, 1017-1025.
Hendrickson, D. G., Hogan, D. J., McCullough, H. L., Myers, J. W., Herschlag, D., Ferrell, J. E. and Brown, P. O. (2009). Concordant regulation of translation and mRNA abundance for hundreds of targets of a human microRNA. *PLoS Biol.* **7**, e1000238.
Hener, P., Friedmann, L., Metzger, D., Chambon, P. and Li, M. (2011). Aggravated TSLP-induced atopic dermatitis in mice lacking dicer in adult skin keratinocytes. *J. Invest. Dermatol.* **131**, 2324-2327.
Hildebrand, J., Rutze, M., Walz, N., Gallinat, S., Wenck, H., Deppert, W., Grundhoff, A. and Knott, A. (2011). A comprehensive analysis of microRNA expression during human keratinocyte differentiation in vitro and in vivo. *J. Invest. Dermatol.* **131**, 20-29.
Hu, H. and Gatti, R. A. (2011). MicroRNAs: new players in the DNA damage response. *J. Mol. Cell. Biol.* **3**, 151-158.
Hu, H., Du, L., Nagabayashi, G., Seeger, R. C. and Gatti, R. A. (2010). ATM is down-regulated by N-Myc-regulated microRNA-421. *Proc. Natl. Acad. Sci. USA* **107**, 1506-1511.
Ito, M., Liu, Y., Yang, Z., Nguyen, J., Liang, F., Morris, R. J. and Cotsarelis, G. (2005). Stem cells in the hair follicle bulge contribute to wound repair but not to homeostasis of the epidermis. *Nat. Med.* **11**, 1351-1354.
Kaufman, C. K., Zhou, P., Pasolli, H. A., Rendl, M., Bolotin, D., Lim, K. C., Dai, X., Alegre, M. L. and Fuchs, E. (2003). GATA-3: an unexpected regulator of cell lineage determination in skin. *Genes Dev.* **17**, 2108-2122.
Lal, A., Pan, Y., Navarro, F., Dykxhoorn, D. M., Moreau, L., Meire, E., Bentwich, Z., Lieberman, J. and Chowdhury, D. (2009). miR-24-mediated downregulation of H2AX suppresses DNA repair in terminally differentiated blood cells. *Nat. Struct. Mol. Biol.* **16**, 492-498.
LeBoeuf, M., Terrell, A., Trivedi, S., Sinha, S., Epstein, J. A., Olson, E. N., Morrisey, E. E. and Millar, S. E. (2010). Hdac1 and Hdac2 act redundantly to control p63 and p53 functions in epidermal progenitor cells. *Dev. Cell* **19**, 807-818.
Lee, J., Basak, J. M., Demehri, S. and Kopan, R. (2007). Bi-compartmental communication contributes to the opposite proliferative behavior of Notch1-deficient hair follicle and epidermal keratinocytes. *Development* **134**, 2795-2806.
Lena, A. M., Shalom-Feuerstein, R., Rivetti di Val Cervo, P., Aberdam, D., Knight, R. A., Melino, G. and Candi, E. (2008). miR-203 represses 'stemness' by repressing DeltaNp63. *Cell Death Differ.* **15**, 1187-1195.
Leung, A. K. and Sharp, P. A. (2010). MicroRNA functions in stress responses. *Mol. Cell* **40**, 205-215.
Lewis, B. P., Burge, C. B. and Bartel, D. P. (2005). Conserved seed pairing, often flanked by adenosines, indicates that thousands of human genes are microRNA targets. *Cell* **120**, 15-20.
Liu, Y. and Liu, Q. (2011). ATM signals miRNA biogenesis through KSRP. *Mol. Cell* **41**, 367-368.

Lynch, M. H., O'Guin, W. M., Hardy, C., Mak, L. and Sun, T. T. (1986). Acidic and basic hair/nail ("hard") keratins: their colocalization in upper cortical and cuticle cells of the human hair follicle and their relationship to "soft" keratins. *J. Cell Biol.* **103**, 2593-2606.
Majid, S., Saini, S., Dar, A. A., Hirata, H., Shahryari, V., Tanaka, Y., Yamamura, S., Ueno, K., Zaman, M. S., Singh, K. et al. (2011). MicroRNA-205 inhibits Src-mediated oncogenic pathways in renal cancer. *Cancer Res.* **71**, 2611-2621.
Mardaryev, A. N., Ahmed, M. I., Vlahov, N. V., Fessing, M. Y., Gill, J. H., Sharov, A. A. and Botchkareva, N. V. (2010). Micro-RNA-31 controls hair cycle-associated changes in gene expression programs of the skin and hair follicle. *FASEB J.* **24**, 3869-3881.
Matsumoto, T., Jiang, J., Kiguchi, K., Ruffino, L., Carbajal, S., Beltran, L., Bol, D. K., Rosenberg, M. P. and DiGiovanni, J. (2003). Targeted expression of c-Src in epidermal basal cells leads to enhanced skin tumor promotion, malignant progression, and metastasis. *Cancer Res.* **63**, 4819-4828.
Millar, S. E. (2002). Molecular mechanisms regulating hair follicle development. *J. Invest. Dermatol.* **118**, 216-225.
Murchison, E. P., Partridge, J. F., Tam, O. H., Cheloufi, S. and Hannon, G. J. (2005). Characterization of Dicer-deficient murine embryonic stem cells. *Proc. Natl. Acad. Sci. USA* **102**, 12135-12140.
Nowak, J. A., Polak, L., Pasolli, H. A. and Fuchs, E. (2008). Hair follicle stem cells are specified and function in early skin morphogenesis. *Cell Stem Cell* **3**, 33-43.
O'Guin, W. M., Sun, T. T. and Manabe, M. (1992). Interaction of trichohyalin with intermediate filaments: three immunologically defined stages of trichohyalin maturation. *J. Invest. Dermatol.* **98**, 24-32.
Oliver, R. F. and Jahoda, C. A. (1988). Dermal-epidermal interactions. *Clin. Dermatol.* **6**, 74-82.
Pan, Y., Lin, M. H., Tian, X., Cheng, H. T., Gridley, T., Shen, J. and Kopan, R. (2004). gamma-secretase functions through Notch signaling to maintain skin appendages but is not required for their patterning or initial morphogenesis. *Dev. Cell* **7**, 731-743.
Paterson, E. L., Kolesnikoff, N., Gregory, P. A., Bert, A. G., Khew-Goodall, Y. and Goodall, G. J. (2008). The microRNA-200 family regulates epithelial to mesenchymal transition. *ScientificWorldJournal* **8**, 901-904.
Peters, E. M., Maurer, M., Botchkarev, V. A., Jensen, K., Welker, P., Scott, G. A. and Paus, R. (2003). Kit is expressed by epithelial cells in vivo. *J. Invest. Dermatol.* **121**, 976-984.
Pierce, A. M., Fisher, S. M., Conti, C. J. and Johnson, D. G. (1998). Deregulated expression of E2F1 induces hyperplasia and cooperates with ras in skin tumor development. *Oncogene* **16**, 1267-1276.
Plikus, M. V., Mayer, J. A., de la Cruz, D., Baker, R. E., Maini, P. K., Maxson, R. and Chuong, C. M. (2008). Cyclic dermal BMP signalling regulates stem cell activation during hair regeneration. *Nature* **451**, 340-344.
Rendl, M., Lewis, L. and Fuchs, E. (2005). Molecular dissection of mesenchymal-epithelial interactions in the hair follicle. *PLoS Biol.* **3**, e331.
Ruby, J. G., Jan, C. H. and Bartel, D. P. (2007). Intronic microRNA precursors that bypass Drosha processing. *Nature* **448**, 83-86.
Ryan, D. G., Oliveira-Fernandes, M. and Lavker, R. M. (2006). MicroRNAs of the mammalian eye display distinct and overlapping tissue specificity. *Mol. Vis.* **12**, 1175-1184.
Selbach, M., Schwanhausser, B., Thierfelder, N., Fang, Z., Khanin, R. and Rajewsky, N. (2008). Widespread changes in protein synthesis induced by microRNAs. *Nature* **455**, 58-63.
Shenoy, A. and Blelloch, R. (2009). Genomic analysis suggests that mRNA destabilization by the microprocessor is specialized for the auto-regulation of Dgcr8. *PLoS ONE* **4**, e6971.
Suzuki, H. I., Yamagata, K., Sugimoto, K., Iwamoto, T., Kato, S. and Miyazono, K. (2009). Modulation of microRNA processing by p53. *Nature* **460**, 529-533.
Tam, O. H., Aravin, A. A., Stein, P., Girard, A., Murchison, E. P., Cheloufi, S., Hodges, E., Anger, M., Sachidanandam, R., Schultz, R. M. et al. (2008). Pseudogene-derived small interfering RNAs regulate gene expression in mouse oocytes. *Nature* **453**, 534-538.
Teta, M., Rankin, M. M., Long, S. Y., Stein, G. M. and Kushner, J. A. (2007). Growth and regeneration of adult beta cells does not involve specialized progenitors. *Dev. Cell* **12**, 817-826.
Vauclair, S., Nicolas, M., Barrandon, Y. and Radtke, F. (2005). Notch1 is essential for postnatal hair follicle development and homeostasis. *Dev. Biol.* **284**, 184-193.
Watanabe, T., Totoki, Y., Toyoda, A., Kaneda, M., Kuramochi-Miyagawa, S., Obata, Y., Chiba, H., Kohara, Y., Kono, T., Nakano, T. et al. (2008). Endogenous siRNAs from naturally formed dsRNAs regulate transcripts in mouse oocytes. *Nature* **453**, 539-543.
Wu, H., Xu, H., Miraglia, L. J. and Crooke, S. T. (2000). Human RNase III is a 160-kDa protein involved in preribosomal RNA processing. *J. Biol. Chem.* **275**, 36957-36965.
Xin, H. B., Deng, K. Y., Shui, B., Qu, S., Sun, Q., Lee, J., Greene, K. S., Wilson, J., Yu, Y., Feldman, M. et al. (2005). Gene trap and gene inversion methods for conditional gene inactivation in the mouse. *Nucleic Acids Res.* **33**, e14.
Xu, N., Brodin, P., Wei, T., Meisgen, F., Eidsmo, L., Nagy, N., Kemeny, L., Stahle, M., Sonkoly, E. and Pivarcsi, A. (2011). MiR-125b, a MicroRNA downregulated in psoriasis, modulates keratinocyte proliferation by targeting FGFR2. *J. Invest. Dermatol.* **131**, 1521-1529.
Yagi, R., Waguri, S., Sumikawa, Y., Nada, S., Oneyama, C., Itami, S., Schmedt, C., Uchiyama, Y. and Okada, M. (2007). C-terminal Src kinase controls development and maintenance of mouse squamous epithelia. *EMBO J.* **26**, 1234-1244.
Yi, R., O'Carroll, D., Pasolli, H. A., Zhang, Z., Dietrich, F. S., Tarakhovsky, A. and Fuchs, E. (2006). Morphogenesis in skin is governed by discrete sets of differentially expressed microRNAs. *Nat. Genet.* **38**, 356-362.
Yi, R., Poy, M. N., Stoffel, M. and Fuchs, E. (2008). A skin microRNA promotes differentiation by repressing 'stemness'. *Nature* **452**, 225-229.
Yi, R., Pasolli, H. A., Landthaler, M., Hafner, M., Ojo, T., Sheridan, R., Sander, C., O'Carroll, D., Stoffel, M., Tuschl, T. et al. (2009). DGCR8-dependent microRNA biogenesis is essential for skin development. *Proc. Natl. Acad. Sci. USA* **106**, 498-502.
Yu, J., Peng, H., Ruan, Q., Fatima, A., Getsios, S. and Lavker, R. M. (2010). MicroRNA-205 promotes keratinocyte migration via the lipid phosphatase SHIP2. *FASEB J.* **24**, 3950-3959.
Zhang, L., Stokes, N., Polak, L. and Fuchs, E. (2011). Specific microRNAs are preferentially expressed by skin stem cells to balance self-renewal and early lineage commitment. *Cell Stem Cell* **8**, 294-308.
Zhang, X., Wan, G., Berger, F. G., He, X. and Lu, X. (2011). The ATM kinase induces microRNA biogenesis in the DNA damage response. *Mol. Cell* **41**, 371-383.
Zhang, Y., Andl, T., Yang, S. H., Teta, M., Liu, F., Seykora, J. T., Tobias, J. W., Piccolo, S., Schmidt-Ullrich, R., Nagy, A. et al. (2008). Activation of beta-catenin signaling programs embryonic epidermis to hair follicle fate. *Development* **135**, 2161-2172.
Zhang, Y., Tomann, P., Andl, T., Gallant, N. M., Huelsken, J., Jerchow, B., Birchmeier, W., Paus, R., Piccolo, S., Mikkola, M. L. et al. (2009). Reciprocal requirements for EDA/EDAR/NF-kappaB and Wnt/beta-catenin signaling pathways in hair follicle induction. *Dev. Cell* **17**, 49-61.

Table S1. Primers used for PCR genotyping of wild-type, floxed and recombined *Drosha* and *Dicer* alleles

Allele	Forward primer (5′ to 3′)	Reverse primer (5′ to 3′)	Product size (bp)
Drosha^{GT} wild type	GATGTGTTGGCAGAAGCTGA [primer (a)]	CCGGAGCACAACACTAATCA [primer (b)]	606
Drosha^{GT} floxed	primer (a)	ACATCATGAAGCCCCTTGAG [primer (c)]	545
Drosha^{GT} recombined	primer (a)	TGCTCAGGTAGTGGTTGTCG [primer (d)]	759
Drosha$^{fl(Ex9)}$ wild type	GCAGAAAGTCTCCCACTCCTA ACCTTC	CCAGGGGAAATTAAACGAGACT CC	251
Drosha$^{fl(Ex9)}$ floxed	GCAGAAAGTCTCCCACTCCTA ACCTTC	CCAGGGGAAATTAAACGAGACT CC	351
Dicer wild type	TCGGAATAGGAACTTCGTTTAA AC [primer (e)]	ATTGTTACCAGCGCTTAGAATT CC [primer (f)]	560
Dicer floxed	primer (e)	primer (f)	767
Dicer recombined	GTACGTCTACAATTGTCTATG [primer (g)]	primer (f)	429